Journal of Molecular Graphics and Modelling 27 (2009) 908–920

Contents lists available at ScienceDirect

Journal of Molecular Graphics and Modelling

journal homepage: www.elsevier.com/locate/JMGM

Modelling β-1,3-exoglucanase–saccharide interactions: Structure of the enzyme–substrate complex and enzyme binding to the cell wall

Sara A. Moura-Tamames, Maria J. Ramos, Pedro A. Fernandes *

REQUIMTE, Departamento de Química, Faculdade de Ciências, Universidade do Porto, Rua do Campo Alegre, 687, 4169-007 Porto, Portugal

ARTICLE INFO

Article history:
Received 10 August 2008
Received in revised form 23 January 2009
Accepted 30 January 2009
Available online 20 March 2009

Keywords:
Retaining glycosidase
Amber molecular dynamics
GOLD covalent docking
Computer modelling
Candida albicans
Protein–polysaccharide interactions
Cell wall binding
Flexible loops

ABSTRACT

Glycoside hydrolases are a class of enzymes that break/form the bond between sugar monomers (monosaccharides). *Candida albicans*'s β-1,3-exoglucanase (Exg), a family 5 glycosidase, belongs to this class of enzymes. This small protein is an ideal computational model for its family of enzymes and was used here to create several enzyme–substrate models starting from a crystallographic glucanase-inhibitor structure. A series of enzyme–substrate complexes were generated using molecular docking, ranging from Exg–glucose (Exg–1Glc) to Exg–laminarihexaose (Exg–6Glc). Structure optimizations followed by molecular dynamics provided a picture of the way the enzyme and substrates interact.

Molecular dynamics was conducted for each complex to assess the flexibility of the substrate, of the enzyme as a whole, and of enzyme–substrate interactions. The enzyme overall conformation was found to be quite rigid, although most enzyme residues increase mobility upon substrate binding. However, two surface loops stand out by having large fluctuations and becoming less flexible when the substrates were bound. These data point to a possible biological role for the mentioned loops, corresponding to amino acids 36–47 and 101–106.

We propose that these loops could bind the enzyme to a glucan chain in the cell wall. The polysaccharide and enzyme structures have very complementary shapes and form numerous interactions; so it appears likely that the flexible loops connect the enzyme to the cell wall and allow it to navigate the wall to shape glucan structure.

1. Introduction

Glycosidases are enzymes specialized in breaking/forming glycosidic bonds between carbohydrate monomers (monosaccharides). They can be divided into two groups regarding their catalytic mechanisms: retaining and inverting glycosidases. Retaining glycosidases maintain the initial conformation (α or β) of the anomeric carbon after hydrolysis of the glycosidic bond; while inverting glycosidases cause a switch to the opposite conformation [1]. There are many experimental studies on the catalytic mechanism used by these enzymes and many crystallographic structures have been obtained [2]. However enzyme–polysaccharide complexes are hard to crystallize, therefore the exact way these proteins bind their substrates, although crucial for a full understanding of the catalytic mechanism, is still very much unknown.

The proposed experimental reaction mechanism of retaining exo-glycosidases is depicted in Scheme 1 [3,4]. The catalytic groups involved are two carboxylic acids, which can be either Asp or Glu residues.

As the substrate enters the binding pocket, the nucleophile residue (bottom) establishes a hydrogen bond with the C_2 hydroxyl group (I). The glycosidic oxygen (O-R) starts dissociating from C_1 simultaneously as it takes the proton from the acid/base catalyst (top). The transition state (TS, II) is reached when the glycosidic bond is almost broken and the nucleophile begins to attack the anomeric carbon (C_1). After this first mechanistic step an enzyme–monosaccharide covalent intermediate is formed and the remaining polysaccharide chain is now free; the proton donor is deprotonated (III). The second mechanistic step of this reaction involves the attack of the monosaccharide–enzyme linkage by a water molecule coupled with a proton transfer from water to the acid/base residue, in a reverse mode of the first step. The final result of the reaction is the hydrolysis of a terminal monosaccharide from the rest of the polysaccharide chain.

The β-1,3-exoglucanase (Exg) enzyme from *Candida albicans* is part of the family 5 glycoside hydrolases [5]. This protein has been chosen as a model for simulating the glycosidase–polysaccharide interactions in this group of enzymes because it is small (400

* Corresponding author. Tel.: +351 220402667; fax: +351 220402659.
E-mail address: pafernan@fc.up.pt (P.A. Fernandes).

1093-3263/$ – see front matter © 2009 Elsevier Inc. All rights reserved.
doi:10.1016/j.jmgm.2009.01.007

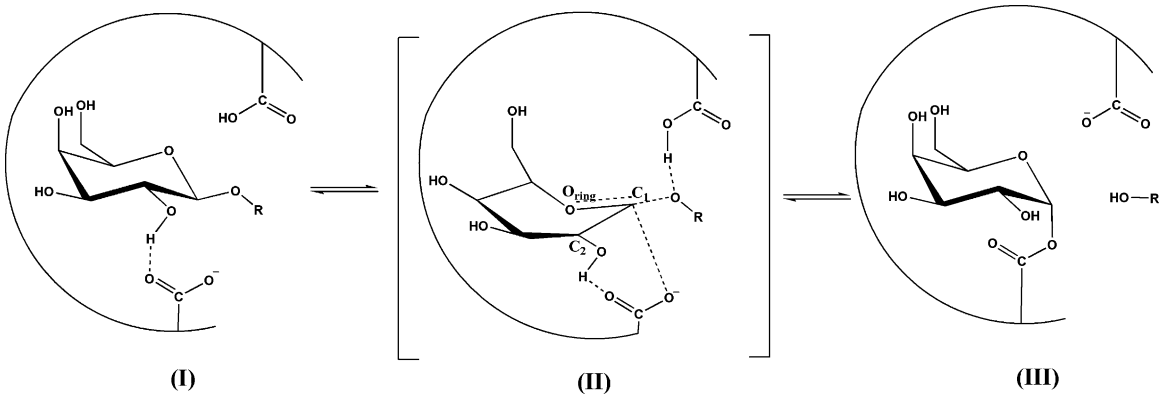

Scheme 1. Reaction mechanism proposed for retaining glycosidases. (I) The formation of the enzyme–substrate complex. (II) Transition state for the first mechanistic step. (III) Products of the first step of the reaction: glycoside–enzyme covalent intermediate and a free polysaccharide chain.

amino acids) and no metal ions are required for maintaining structure stability. There are several crystallographic structures of this protein with a good resolution available in the Protein Data Bank (PDB) [6]: an unbound enzyme structure (1CZ1) as well as two structures of the protein bound to different inhibitors: a transition state analogue (1EQC) and a mechanistic inhibitor (2PB1) [7].

Exg is a retaining glycosidase that specifically binds β-1,3 linked glucose residues (laminarin series—see Scheme 2) in the catalytic pocket [8]. It can both hydrolyze the 3-terminal glucose residue of a polylaminari-chain (glycoside hydrolysis) or remove that residue from one chain and then add it to another chain on its 3-terminal (transglucosylation). The catalytic amino acids are Glu292 (nucleophile) and Glu192 (acid/base catalyst). This protein is present in the cell wall and it is believed to be involved in β-Glucan reorganization. β-Glucan is a homopolymer of glucose units bound by β-1,3 linkages with occasional β-1,6 ramifications; it is the main constituent of the cell wall of *C. albicans* [9]. However, unlike most proteins that act within the cell wall, there is no experimental evidence of the exoglucanase being glycosylated [10]. How it is able to bind and stay within the wall (escaping diffusion to the extracellular space) is therefore unknown.

C. albicans is an important human pathogen causing infections in several areas of the body, in particular mucosae, the gastro-intestinal track and the skin. Widespread *C. albicans* strains are becoming increasingly resistant to generally used anti-fungal drugs such as Fluconazole [11]. The Exg gene, although not essential for the survival and pathogenicity of this fungus, is important in conferring resistance to antifungal agents [12]. Any disruption to the cell wall structure resulting from low levels of exoglucanase activity could reduce *C. albicans* survival to antifungals. The inhibition of this enzyme concomitantly with antifungal therapy could respond to the problem of highly resistant strains. A greater understanding of the mechanism of action of this enzyme can provide a basis for the development of new, very specific antifungal drugs, since there is no human parallel to the Exg gene.

2. Methodology

The generation of the periodic solvent box and all minimizations, molecular dynamics and dynamics results analysis were conducted using the Amber 8 suite of programs [13]. The ff99 force field in conjunction with the glycam04 force field (for carbohydrates) was used in all calculations [14]. Graphical displays were generated with the Discovery Studio Visualizer 2.0 from Accelrys Software Inc.

2.1. Energy minimization and protonation state of the enzyme

The crystallographic structure of β-1,3-exoglucanase free of ligands (1CZ1) [7] with a resolution of 1.85 Å was used as a starting structure for the study of the free enzyme. Charges were neutralized by adding Na^+ counter-ions and the structure was solvated with a 12 Å truncated octahedron periodic water box using the tleap program from the Amber 8 suite [13]. During this study, the protonation states of some amino acids were found to be important for catalysis and for maintaining enzyme structure. Therefore, standard protonation states were used for all amino acids except the following:

– His135 was protonated on both ring nitrogens (positively charged) (HIP in Amber nomenclature).

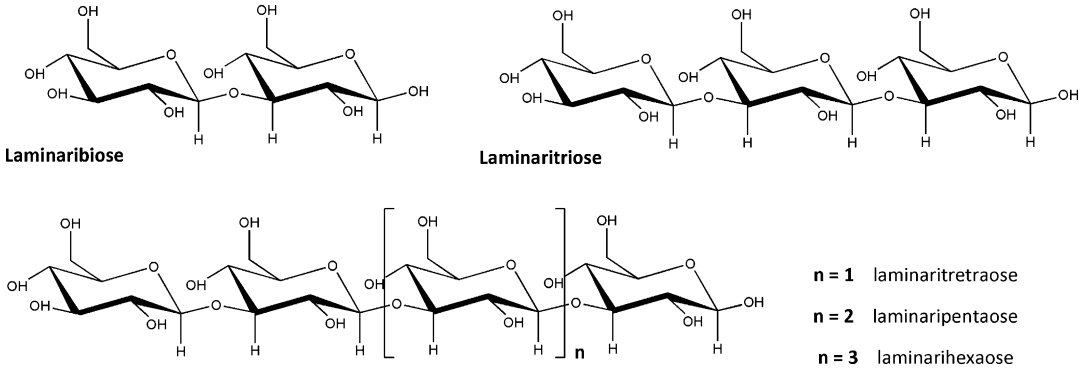

Scheme 2. 2D structure of the oligosaccharides modelled as substrates for the Exg enzyme.

– His253 was protonated on the δ nitrogen (HID).
– Asp251 and Glu192 were protonated (ASH and GLH).

Next, the energy of the system was minimized. This procedure was repeated for every enzyme–substrate complex modelled.

Energy minimizations were conducted in three stages. A cutoff of 12 Å was used for all minimizations. In the first minimization all protein and substrate residues were restrained with a 500 kcal mol^{-1} A^2 force constant. 500 minimization cycles were run using the steepest descent method after which the conjugate gradient method was used for 500 more cycles. In this way the water molecules were allowed to relax to some extent around the enzyme.

In the second minimization only the backbone carbons of the protein were restrained with the same force constant as before. 5000 steepest descent cycles were run followed by 5000 conjugate gradient cycles. In the third minimization no restraints were used, and the number of cycles was the same as in minimization 2.

2.2. Generating Exg–substrate complexes

The β-1,3-exoglucanase:castanospermine complex (Exg–cast, 1EQC) [7] was used as a starting structure for the design of the glucanase–glucose complex (Exg–1Glc). Castanospermine is a glucose analogue, so it was simply necessary to replace/add a few atoms using Discovery Studio Visualizer 2.0 to convert castanospermine into a glucose molecule (Supporting Information: Scheme SI1). The Glucanase–1Glc initial complex was treated as mentioned above, and its geometry was optimized.

To generate the several enzyme–oligosaccharide complexes the following procedure was used. The previously minimized Exg–substrate complex was stripped of water molecules and ions and saved using the pdb format. A new glucose residue was then added to the last glucose residue previously bound to Exg using the docking software GOLD 3.1 [15,16]. The default docking settings were used with a few exceptions, explained next. The protein–substrate complex was considered as a unit on to which the new glucose residue would be bound. GOLD 3.1 was used with the Chemscore algorithm to screen for different binding modes of this glucose residue, attempting to maximize the interactions formed between the added glucose residue and the enzyme–substrate structure, generating several possible protein–ligand complexes. The covalent docking option was chosen, determining that a β-1,3-glycosidic bond had to be formed between the glucose residues, in order to generate the intended polysaccharide chain [17,18]. Ten possible solutions were then obtained. The option for early termination of the docking if very similar results were obtained for the first structures generated was turned off. This allowed different structures to be generated and evaluated visually, choosing the best one according to the enzyme function and mechanism, instead of relying only on an automated procedure to choose the best result.

The enzyme–substrate complex generated in this way was then solvated and neutralized as described before, and its energy minimized. This procedure was repeated several times, resulting in the addition of glucose residues one by one to the previously optimized enzyme–substrate complex. Complexes of Exg bound to substrates glucose (1Glc), laminaribiose (2Glc), laminaritriose (3Glc), laminaritetraose (4Glc), laminaripentaose (5Glc) and laminarihexaose (6Glc) were created. 2D structures of these polysaccharides are presented in Scheme 2. The optimized structures were analyzed with Discovery Studio Visualizer 2.0 and subsequently used as a starting point for molecular dynamics.

2.3. Molecular dynamics

All enzyme–substrate complexes and free enzyme dynamics were conducted using the same method. The SHAKE algorithm [19] and Langevin thermostat [20] were used. The cutoff of 12 Å was maintained. The equilibration phase had two stages. To avoid possible system instability caused by the automatic generation of initial velocities for its atoms, the system was first heated from 200 to 310.15 K (body temperature-enzyme optimum) during 10 ps, with constant volume. The protein and substrate were restrained with a 10 kcal mol^{-1} A^2 force constant. Subsequently, constant pressure at 1 bar was employed, maintaining the temperature at 310.15 K for an additional 90 ps. Charts for temperature (T), potential energy (E_p) and rmsd vs. time were created for the equilibration stage; these values became stable after just 20 ps, which indicated that the system had reached an equilibrium stage. Following the equilibration, the production phase was initiated using the same parameters as in the second equilibration stage and run for 1000 ps (1 ns). Graphs for T and E_p were also generated for the production, to confirm the system maintained its stability.

2.4. Molecular dynamics analysis

VMD for win32 version 1.8.6 [21] was used to observe the trajectories and save coordinate files as pdb files. The ptraj utility of the Amber suite of programs was used to calculate the root mean square deviations (rmsd) and root mean square fluctuations (rmsf) of the enzyme and substrates. Rmsds were calculated for the free enzyme and all complexes, with mass-weighting and using the first structure of the run as the reference. In addition, rmsds were determined using the initial crystallographic structures as reference for the free enzyme (which was compared to 1CZ1) and the Exg–6Glc complex (which was compared to 1EQC). The rmsfs were calculated by residue for enzyme structures and by atom for substrate molecules.

2.5. Modelling loops–polysaccharide interaction

After analysing the previous results, we decided to study a possible interaction between the enzyme loops formed by amino acids 36–47 and 101–106 and a polysaccharide chain of the laminari-series. A polysaccharide with 18 glucose residues linked by β-1,3-glycosidic bonds (18Glc) was built using the Glycam web site [22]. This ligand was then placed manually between the two mentioned loops of the enzyme, sitting in the groove that exists between the loops. Discovery Studio Visualizer 2.0 was used to represent and move the molecules during this process. No change in conformation was made in either the enzyme or 18Glc, yet the two macromolecules had a remarkable complementarily. Different states of the enzyme were used for modelling an enzyme:18Glc complex: Free Exg (at 700 ps of production, after a conformational switch occurred), Exg–6Glc and Exg–1Glc (both at 500 ps, the midpoint of dynamics).

To predict the interactions between the enzyme and ligand, a similar energy minimization procedure was used for every enzyme–ligand system created (Exg:18Glc, Exg–6Glc:18Glc and Exg–1Glc:18Glc). Following charge neutralization, the system was solvated with a 16 Å truncated octahedron periodic water box. Three minimizations were run sequentially, and a cutoff of 14 Å was used for all of them. In the first minimization, enzyme, ligand (and substrate) were restrained with a 500 kcal mol^{-1} A^2 force constant so the water molecules could relax around the enzyme and the polysaccharide(s). 10,000 minimization cycles were run, the last 5000 being conjugate gradient cycles. For the second and third minimization, 20,000 cycles were run and after 5000 of steepest descent cycles, conjugate gradient cycles were used. In the second

minimization only the α-carbons of the protein were restrained, whereas in the last minimization no restraints were used.

3. Results and discussion

Our aim in this study was to create a reliable enzyme–substrate model for family 5 glycosidases (and possibly for related families), using *C. albicans* β-1,3-exoglucanase experimentally determined enzyme and enzyme–inhibitor (Exg–cast) structures. After transforming castanospermine into glucose, the Exg–1Glc model was obtained. Five more glucose residues were added by docking the monomers one by one into the previously obtained enzyme-bound oligomer, forming a covalent β-1,3 linkage. The several structures obtained (Exg, Exg–1Glc, Exg–2Glc, Exg–3Glc, Exg–4Glc, Exg–5Glc and Exg–6Glc) were optimized by minimizing their energy. Subsequently, enzyme–substrate interactions were analyzed for all the complexes.

3.1. Enzyme–substrate structure after optimization

Glucose ring numbering and conformations are illustrated for glucoses 1 and 2 in Fig. 1a. In Fig. 1b the overall structure of the laminarihexaose substrate molecule bound to the glucanase is shown. Glucose residues were numbered 1–6 starting from the free 3-terminal; so glucose 1 is the glucose residue bound in the reaction pocket (subsite −1) and glucose 6 is the residue bound at the other end of the binding groove (subsite +5). A free glucan chain is predicted to have a twisted linear structure, with strong H bonds between neighbouring glucose residues [22]. The polysaccharide chain was distorted in binding the enzyme, but many of the intramolecular hydrogen bonds were maintained.

Independently of which substrate was considered, the interactions originated between the amino acid residues forming a given enzyme binding subsite and the glucose residue it bound were identical. Therefore, the enzyme appears to bind a given glucose residue the same way, regardless of the substrate length. The different substrates were superimposed and it was verified that the variations in the conformations of the glucose residues were minimal. Therefore, results will only be presented for the Exg–6Glc complex, used as an example (Fig. 1c).

The Exg enzyme breaks the glycosidic bond between glucoses 1 and 2; these glucoses were held by several amino acids residues and their structure and orientation appears to be shaped by the interactions established. This is probably essential for reaction catalysis. Observing Fig. 1b we can see that the binding of the two 3-terminal glucose residues by the enzyme caused a loop-like distortion in the substrate chain. This positioning is expected to favour reaction progression, because it places the anomeric carbon in a more favourable way to be attacked after the dissociation of the glycosidic bond.

Glucose 1 was observed to be strongly bound to the enzyme by 6 short hydrogen bonds (Fig. 1c). These interactions, made with Glu27 (2 H-bonds), Tyr29, His135, Asn191 and Glu292, appear to maintain its structure in a half-chair conformation (Fig. 1a). This distortion should be important for catalysis since it brings the glucose residue closer in geometry and, consequently, in energy to the TS. The transition state is believed to proceed through a half-chair conformation [1,2,4] therefore a distortion of the glucose ring upon binding would facilitate the evolution to the TS quickly after the formation of the enzyme–substrate complex [4]. One can, however, wonder: why should the glucose residue bind the enzyme to be thus distorted when it could be in a relaxed conformation and also establish H-bridges whilst solvated? The difference in energy between the chair conformation and the half-chair conformation observed here is 5.8 kcal mol^{-1} [23]. The chair conformation is unlikely to occur in the −1 subsite (when positioned as observed in the enzyme-complexes created), due to likely collision with some amino acids (namely His135) and impaired interaction with other amino acids. Therefore, for the substrate to bind the enzyme, the energy of the interactions thus established should outweigh the energy barrier required to alter the chair glucose ring to the half-chair conformation (which is less than 8 kcal mol^{-1} [23]). A typical water:glucose (O···H) hydrogen bond is about 2 Å in length, while the H bonds established between glucose 1 and the enzyme are in general much shorter and therefore stronger. The negatively charged oxygens of the active site glutamates and also histidine positive charge result in stronger electrostatic binding (ion–dipole interactions). In addition, the enzyme residues are positioned to balance the electrostatic surface of the glucose ring and favour the adoption of the half-chair conformation.

The enzyme–substrate interactions established in the binding pocket appear to be specific and to depend not only on the interacting amino acids residues but also on their correct orientation by other amino acids residues *via* hydrogen bonds, as displayed in Fig. 1d. During our study, we verified that if these hydrogen bonds did not form due to the use of incorrect protonation states for some amino acids residues, then the catalytic residues would bind the substrate in an unexpected way, which was unlikely to favour the reaction.

The second glucose ring was secured between two Phe aromatic rings: Phe144 and Phe258 (Fig. 1c), as predicted by Cutfield et al. [7]. Besides these London interactions, a hydrogen bond to the proton donor (Glu192) was observed. The two phenylalanine residues seem to orient the second glucose residue in a way that positions its C_2–OH group close to the acid/base catalytic residue; and the hydrogen bond created between them could be important to facilitate reaction progression. Although not shown in Fig. 1c, the rest of the C–OH groups of this glucose residue are also involved in hydrogen bonds, either with water molecules or with neighbouring glucose residues (see Fig. 1b). Consequently, we can expect that this second residue binding to the enzyme is a favourable process, since it retains most intramolecular H bonds as well as those it established with water molecules when in solution, and it gains ring-to-ring interactions with two Phe residues. In contrast with the first glucose residue, the second glucose is in a relaxed chair conformation, and no ring strains are imposed by interacting with the protein (Fig. 1a).

The latter glucose residues are not involved in the reaction (glucoses 3–6) and were bound to the enzyme in a less specific way. They appear to have more freedom of movement, since they only interact with Exg using one side of the ring. The binding groove provides this effect, since it is mainly hydrophobic on one side and mainly hydrophilic on the other side (Supporting Information: Scheme SI2). Glucoses 3–6 interacted with the hydrophilic side of the groove by hydrogen bonds. It is interesting to note that most bridges were established with the backbone of the protein instead of amino acid side-chains, and two conserved residues (His253 and Tyr255) appear to be involved in this kind of interactions. The Tyr255 side chain is additionally important for maintaining structural stability in the core of the binding pocket. Any attempt to change the conformation of this amino acid resulted in a great disruption of enzyme structure during energy minimization (results not shown).

3.2. Comparison to enzyme–inhibitor structures

After the generation and energy minimization of the several enzyme–substrate complexes, molecular dynamics was conducted for all the complexes as well as for the free enzyme. This provided a better picture of the structure and stability of the Exg–substrate complexes.

(a)

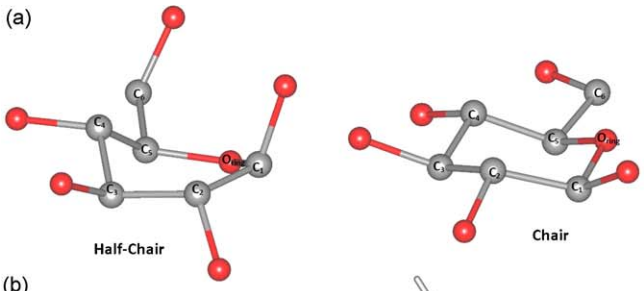

(b)

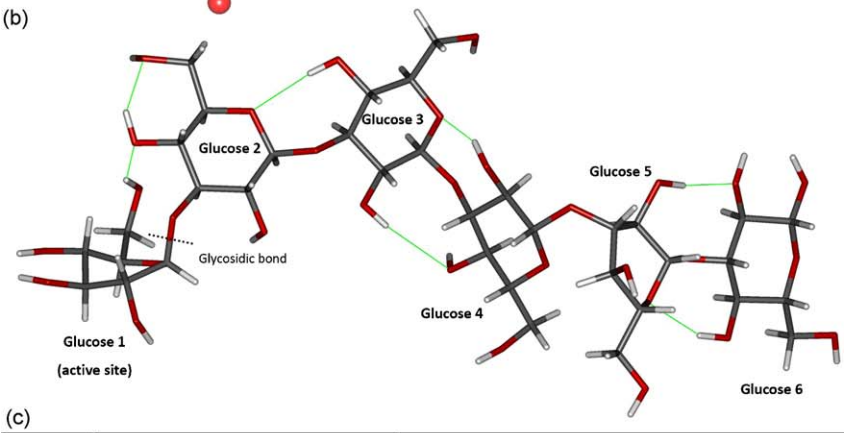

(c)

Glucose residue	Interacting enzyme residues		Image
	residue	*interaction*	
1	Glu27	-O...HO-C3 and -O...HO-C4	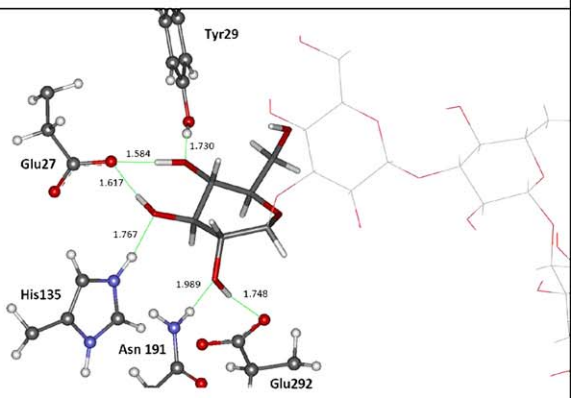
	Tyr29	-OH...OH-C4	
	His135	ring-NH...OH-C3	
	Asn191	-NH....OH-C2	
	Glu292	-O...HO-C2	
2	Glu192	-OH...OH-C2	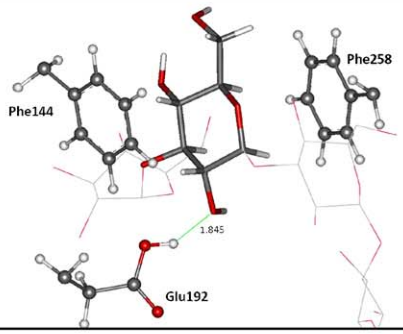
	Phe144	aromatic ring...glucose ring	
	Phe258	aromatic ring...glucose ring	
3	Glu262	-O...HO-C6	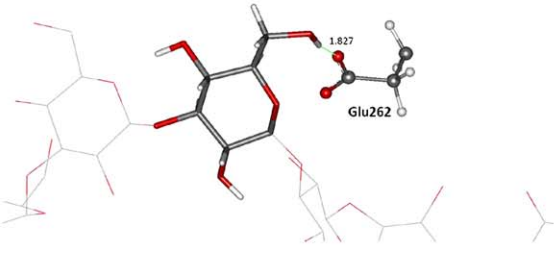

(d)

a.a. residue	Orienting interactions	Image
Arg92	NH...O-Glu292 and NH...O-Ans191	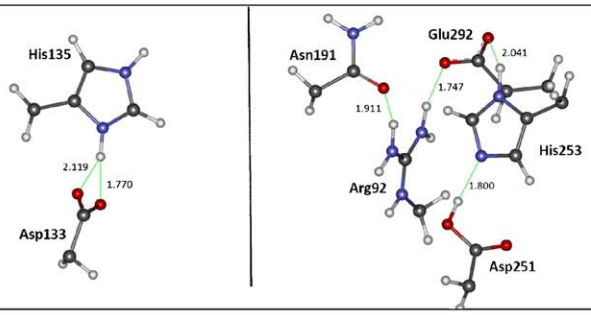
Asp133	O...HN-His135	
Asp251	OH...His253	
His254	NH...O-Glu292	

(e)

Glucose residue	Interacting enzyme residues		Image
	residue	*interaction*	
4	His253	Mainchain-C=O...HO-C6	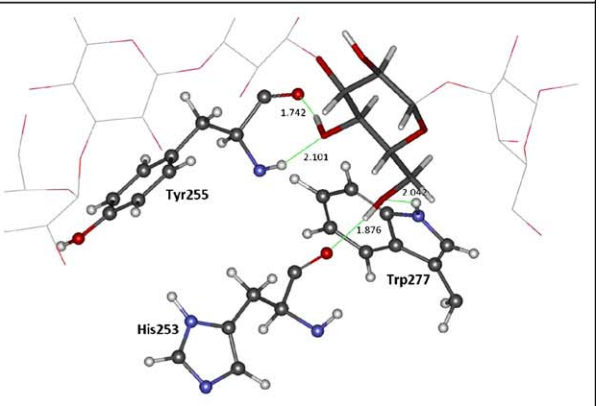
	Tyr255	Mainchain-C=O...HO-C4 Mainchain-N-H...HO-C4	
	Trp277	ring-NH...OH-C6	
5	Gln230	Mainchain-C=O...HO-C4	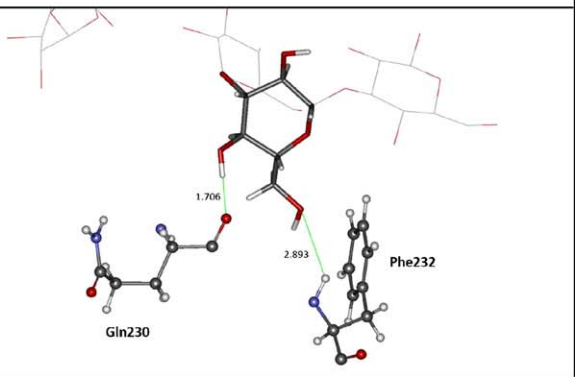
	Phe232	Mainchain-NH...OH-C6 (weak)	
6	Asn276	-C=O...HO-C6	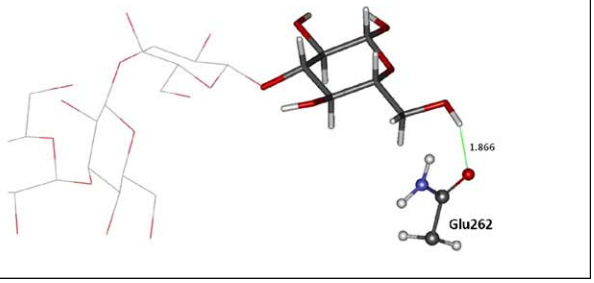

Fig. 1. (*Continued*).

Fig. 1. (a) The glucose ring carbon numberings and conformations. On the left is the first glucose residue of the laminarihexaose chain, in the half-chair conformation and on the right the second glucose residue which is in a perfect chair conformation. Hydrogen atoms were omitted for clarity. (b) Overall conformation of laminarihexaose when bond to Exg. Several intramolecular hydrogen bonds are formed. The glucose numbering used in this work and the glycosidic bond hydrolyzed by the enzyme are also shown. (c) Specific interactions established between the three 3-terminal glucose residues of laminarihexaose and 1,3-exoglucanase. (d) Interactions made between residues of the protein that orient residues His135, Ans191 and Glu292, which interact with the substrate. (e) Interactions found between the enzyme and glucose residues 4, 5 and 6 of laminarihexaose. Note that many contacts are made with the backbone of the protein. *Remark*: (c), (d) and (e) refer to the Exg–6Glc structure after energy minimization.

To validate our model of the enzyme–substrate complexes we thought it convenient to compare the results obtained with the PDB structures of the enzyme–inhibitor complexes available. The last dynamics structure (1000 ps) of the Exg–2Glc complex was used. The Exg–cast complex had a very similar structure to the Exg–2Glc, as expected. The rmsd (root mean square deviation) gives a measure of how much the corresponding atoms of two different structures of the same molecule differ in position from each other; the value obtained is an average for all the molecule's atoms. In this case, the rmsd between the modelled Exg–2Glc and the experimental Exg–cast was calculated to be only 1.26 Å, illustrating how similar the two structures were. This confirms that the model created was stable and did not diverge from the initial structure during the dynamics run.

A complex of Exg bound both to 2-deoxy-2-fluoro-glucose (2F-Glc) and 2,4-dinitrophenyl-2-deoxy-2-fluoro-β-D-glucopyranoside (2F-Glc-DNTP) is available on the PDB (2PB1) [7]. The 2F-Glc is linked covalently to the nucleophile as the result of the enzymatic hydrolysis of a 2F-Glc-NTP molecule (acting as a mechanistic inhibitor) and will not be considered here. A second 2F-Glc-DNTP molecule is bound non-covalently to the enzyme, between Phe144 and Phe258. Accordingly, this location was proposed to be the binding site for the second glucose residue of the substrate [7]. As described above, in our model the second glucose ring is bound as anticipated, in a very similar way to how the 2F-Glc-DNTP binds (Fig. 2). The rmsd between Exg–2Glc and the enzyme bound to these two inhibitor molecules is small (1.16 Å), further confirming the accuracy of the enzyme–substrate model created. The Phe residues changed little in position between the two structures. Note that although the inhibitor glucose ring seems to be better accommodated between the two aromatic rings, it is because its position is not constrained by a glycosidic bond to the first glucose, as occurs in the substrate. This enzyme–inhibitor complex is thus a better approximation for the products of the first mechanistic step than for its reactants.

3.3. Rmsd and visual observations during the dynamics run

The rmsd was calculated relative to the initial structure of the production phase for all complexes during the total 1000 ps that comprise this stage, and is shown in Fig. 3a. From 0 to 200 ps, the rmsd steadily increased as the enzyme structure deviated from its initial structure. After 200 ps, the rmsd was reasonably stable for all complexes, at around 1.2 Å. These small rmsd values represent a fairly rigid enzyme, which changes little in conformation over time.

The free enzyme rmsd is very similar to the rmsd of the enzyme–substrate complexes, although it seems to have a sudden change of conformation at about 650 ps, corresponding to a small jump in the rmsd value, which then becomes stabilized at this figure for the rest of the dynamics procedure. The VMD graphics program was used to observe enzyme movements over time and compare its structures both before and after the 650 ps jump. We noticed that the overall enzyme structure appeared constant over time, except for a loop on the enzyme surface composed of amino acids 36–47 that changed conformation after the 650 ps mark. In the enzyme–substrate complexes this loop showed much smaller changes in structure. The importance of these findings will be discussed further in Section 3.5.

The rmsd of the substrate molecules is also shown in Fig. 3a. The small substrates were practically immovable, whereas the larger substrates tended to have greater position changes. The small variations registered in the rmsd of the enzyme in complex increased with substrate size, and probably reflect the enzyme accommodating the conformational changes of the substrate. We can observe that small substrates (1Glc–3Glc) moved little over time, which is in accord with the tight binding the enzyme provides to glucose residues 1 and 2. When a fourth or more glucose residues were added, the substrate as a whole moved much more, and this was due to the shifts of the latter glucose residues.

The substrate molecular movements were observed with VMD over the production time and we noticed that the last glucose residue in the longer chains (4Glc to 6Glc) rotated around the glycosidic bond, causing smaller rotations in the previous glucose residues. The first two glucose residues were nonetheless very stable, and were not particularly affected by the movements of other residues.

Simultaneously as the glucose residues 4–6 rotated, they seemed to somewhat disengage from the enzyme groove as they became better solvated, and established more intramolecular H-bonds. The rotation of the substrate chain that occurred during the dynamics is probably due to the method used to create the enzyme–substrate complexes. The one-by-one glucose docking procedure probably originated a small distortion of the overall laminari-chain relative to its most stable conformation in the attempt to maximize the

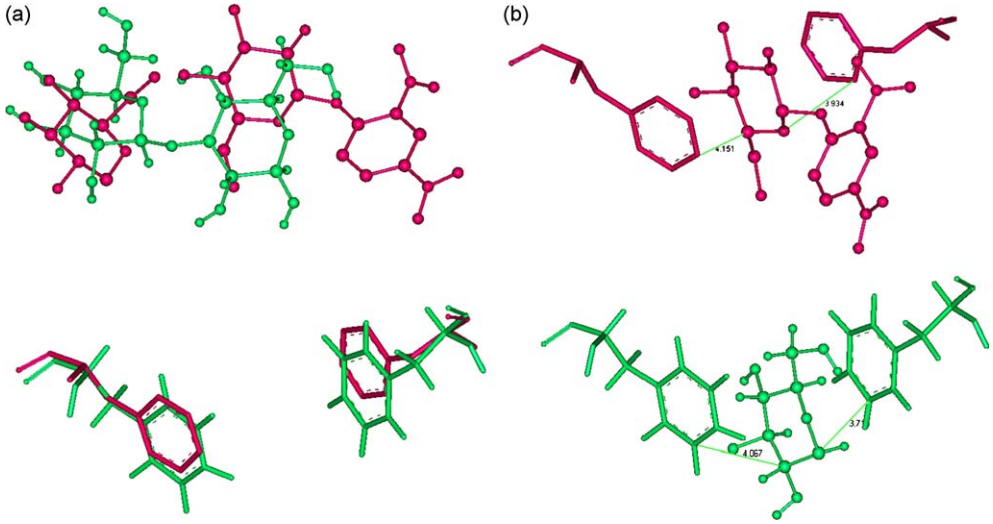

Fig. 2. (a) Superimposition of Exg-2F-Glc-DNTP (pink) and Exg–2Glc (green) structures. TOP: laminaribiose/inhibitor position. Bottom: Phe144 and Phe258 positions. (b) Interactions between ligand and enzyme. Top: Exg–inhibitor complex. Bottom: Exg–2Glc complex. *Note:* only the glucose residue/inhibitor bound at the +1 subsite is shown for simplicity.

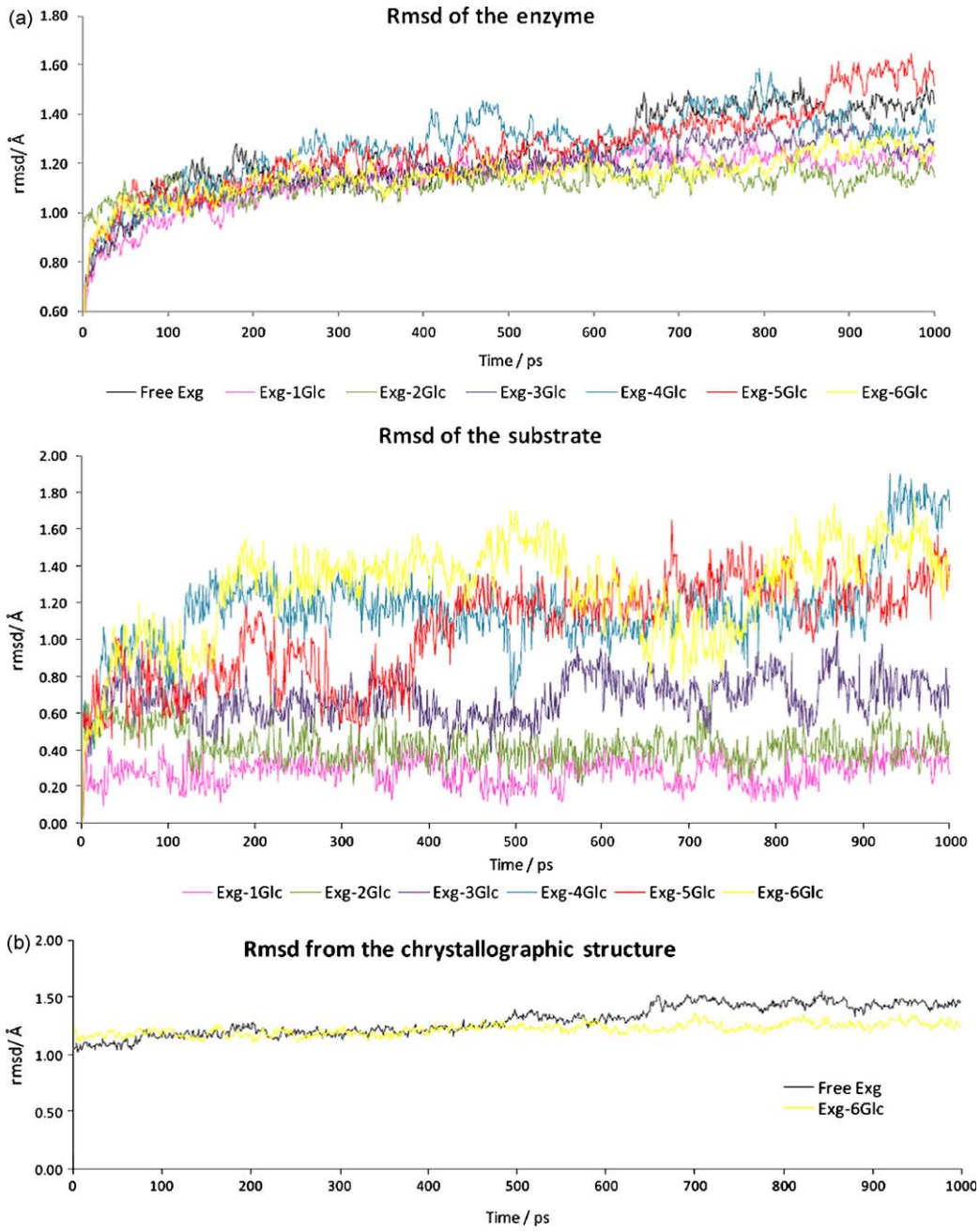

Fig. 3. (a) Rmsd of the enzyme (top) and the substrate (bottom) in the different complexes during the 1000 ps production phase using the initial structure of this stage as reference. (b) Rmsd of the protein for the free enzyme and the Exg–6Glc complex using the crystallographic structures for the free enzyme (1CZ1) and the Exg–castanospermine complex (1EQC), respectively, as reference.

interactions with the enzyme. This caused the substrate to coil to a more stable conformation during the dynamics run.

With the purpose of analysing the stability of the enzyme–substrate interactions observed after the energy minimization, we assessed the amino acids and interactions mentioned in Fig. 1c–e during the dynamics run. Once again, the results were very similar for all the complexes and the following observations are general when not otherwise specified.

All enzyme interactions with glucose 1 were very stable, with a constant conformation of the amino acids and the glucose residue involved; except for the interaction with Asn191 which disappeared during the equilibration stage as the amino acid residue moved away from the substrate. This conformation change is probably due to a relaxation of the enzyme structure during the dynamics, which was not possible during the minimization due to the smaller conformational variations possible. This lost interaction should therefore not be very significant to the enzyme–substrate binding and reaction mechanism. During the production phase this asparagine moved further away from the substrate and rotated approximately 180 degrees along the C_α–C_β bond; however it maintained hydrogen bonding interactions with Arg92 most of the time. The new position adopted by Asn191 allowed it to interact additionally with Asp251 (hydrogen bonds).

The position of the other orienting amino acids shown in Fig. 1d changed little during the dynamics and the interactions observed between them were maintained. Histidines are well known for their role in charge stabilization in various reaction mechanisms [24], and the two histidines present in the active site could have this role. His135 binds the substrate and is linked to Asp133 by two hydrogen bonds, a typical charge transfer system. His253 is

Table 1
Average root mean square deviation from the initial production structure for the last 800 ps of the production phase for the enzyme ($Rmsd_{enzyme}$) and substrate ($Rmsd_{substrate}$).

$Average_{200-1000ps}$	Exg	Exg–1Glc	Exg–2Glc	Exg–3Glc	Exg–4Glc	Exg–5Glc	Exg–6Glc
$Rmsd_{enzyme}$	1.288	1.188	1.132	1.220	1.328	1.318	1.181
$Rmsd_{substrate}$	–	0.289	0.409	0.691	1.212	1.132	1.342
$Rmsd_{crystallography}$	1.337	–	–	–	–	–	1.232

$Rmsd_{crystallography}$ is the rmsd when the crystallographic structure is used as reference.

conserved in the family 5 hydrolases [7], and is bound to an aspartate (Asp251), these residues, together with Arg92 (which is also conserved) and Asn191 could be involved in a charge transfer system that would guide the attack of the nucleophile on the substrate and stabilize the covalent intermediate.

Now we can propose that the active site is well adapted to conduct the substrate rapidly to the transition state, not only altering its conformation to facilitate the nucleophilic attack, but also accommodating the excess of positive charge generated at the anomeric carbon and the endocyclic oxygen as the glycosidic bond (one of the most stable bonds in nature) is broken.

The interactions between glucose 2 and the enzyme were constant during the entire dynamics run; however the interactions with latter glucose residues changed as the dynamics progressed. The interaction between Glu262 and the third glucose was fairly stable, although it was broken near the end of the dynamics for complexes Exg–4Glc and Exg–6Glc, because the C_6 of glucose 3 changed its position.

Glucose 4 interacted mainly with the backbone of the protein, but with different residues over time, as it changed its position. The interaction with the backbone of His253 was maintained during the Exg–4Glc dynamics and also during most of the Exg–6Glc dynamics, although it was lost in Exg–5Glc complex. The hydrogen bond interaction with the Trp277 ring was lost early (during the equilibration) as the glucose moved away from this residue.

The fifth glucose residue also presented changeable hydrogen bonds with backbone atoms and the interactions observed after the minimization were lost, while other connections were formed. A stable interaction with the sidechain of Asp280 was also formed.

Glucose 6 interacted with Asn276 during most of the dynamics run, before it rotated and lost contact with this amino acid. Several interactions with the backbone of the protein were also observed over time. The position of this residue seemed to be more stable than that of the 1-terminal residues of laminaripentose and laminaritetrose, presenting less rotation over the glycosidic bond. An arginine residue (Arg265) became close to glucose 6 during the dynamics run and a strong ion–dipole interaction seemed to be established between them.

Glucose residues 4–6 most likely interact with the binding groove in a fluid way, changing their position and connections over time. It is probable that the groove connected to the binding pocket does not serve to strongly bind the substrate chain during the reaction. This groove may have a different role: to facilitate the formation of the enzyme–substrate complex. The groove could engage a glucan chain through its free 3-terminal and direct it to enter the binding pocket, where it then becomes locked. The hydrophobic/hydrophilic nature of the groove could easily provide a "slide" (in a way similar to the greasy slide of bacterial porins for oligosaccharides [25]): the substrate could rapidly shift along the numerous H-bond interaction sites provided by the backbone atoms until it reaches the two-Phe gate and interacts with the enzyme pocket, where it becomes locked until the glycosidic bond is broken. Then, the main part of the glycosidic chain could easily disengage the enzyme while the protein covalently held the last glucose residue. The sliding groove would subsequently facilitate the association of the glucanase to another glucan chain to which it could link the glucose residue in a transglucosylation reaction. Experimental reaction rate measurements indicate that the main function of this enzyme is transglucosylation rather than hydrolysis, supporting this view [8].

To further validate the enzyme–substrate models created, we also calculated the rmsd over the production time comparing the dynamics structures with the crystallographic structures available (Fig. 3b). The free enzyme was compared to the initial free enzyme PDB structure and the Exg–6Gcl complex was compared to the Exg–cast PDB structure, the best approximation to an enzyme–substrate complex. The resulting rmsds were very small and constant over time, so we can state that the dynamics structure did not diverge from the experimentally determined structure. The rmsd for the substrate complex was particularly stable, which indicates that neither the modelling procedure nor the binding of a large substrate altered significantly the structure of the enzyme.

A table summarizing the results is presented (Table 1) displaying the average rmsds for all the structures over the last 800 ps of the dynamics run, since it was the most stable during this time. The average enzyme rmsd relative to the initial production structure varied between 1.181 Å for Exg–6Glc and 1.328 Å for Exg–4Glc. The values are small and vary little between the different complexes, as already stated. It is interesting to note that the smallest value occurs for the enzyme–laminarihexaose complex, probably a result of the stronger interactions the enzyme made to the last glucose residue in this case, reducing the movement of the substrate chain. Observing the very small rmsd values for substrates 1Glc–3Glc we note how little these substrates move, being held by the enzyme. When the fourth glucose is added the rmsd almost doubles from the one in Exg–3Glc, indicating that the later glucose residues have greater mobility and produce this large increase in the average displacement of the entire molecule from its initial structure. The root mean square deviation from the crystallographic structure is similar to the values obtained for the rmsd relative to the initial production structure, authenticating our model. The rmsd relative to the experimental structure is also smaller for the Exg–6Glc than for the free enzyme.

3.4. Rmsf during the dynamics run

The root mean square fluctuation (rmsf) is a measure of the displacement of an atom (or group of atoms) around its average position during a defined period of time; it provides an assessment of the rigidity of different parts of a molecule.

First we analyse the rmsf per atom of the substrate, shown in Fig. 4a. The atoms corresponding to each glucose residue are shown in the chart. Atoms belonging to the sugar ring and groups linked to ring carbons are rigid, due to the restricted movement of the ring. For every glucose unit there is a peak in flexibility corresponding to the C_6–OH group which is out of the ring and consequently has a greater conformational flexibility.

We can also see in the graph that the first two glucose residues show very limited movement (with rmsf values between approximately 1 and 1.5 Å) due to the way the surrounding enzyme residues interact with these substrate residues. This agrees with previous observations: the enzyme securely holds the

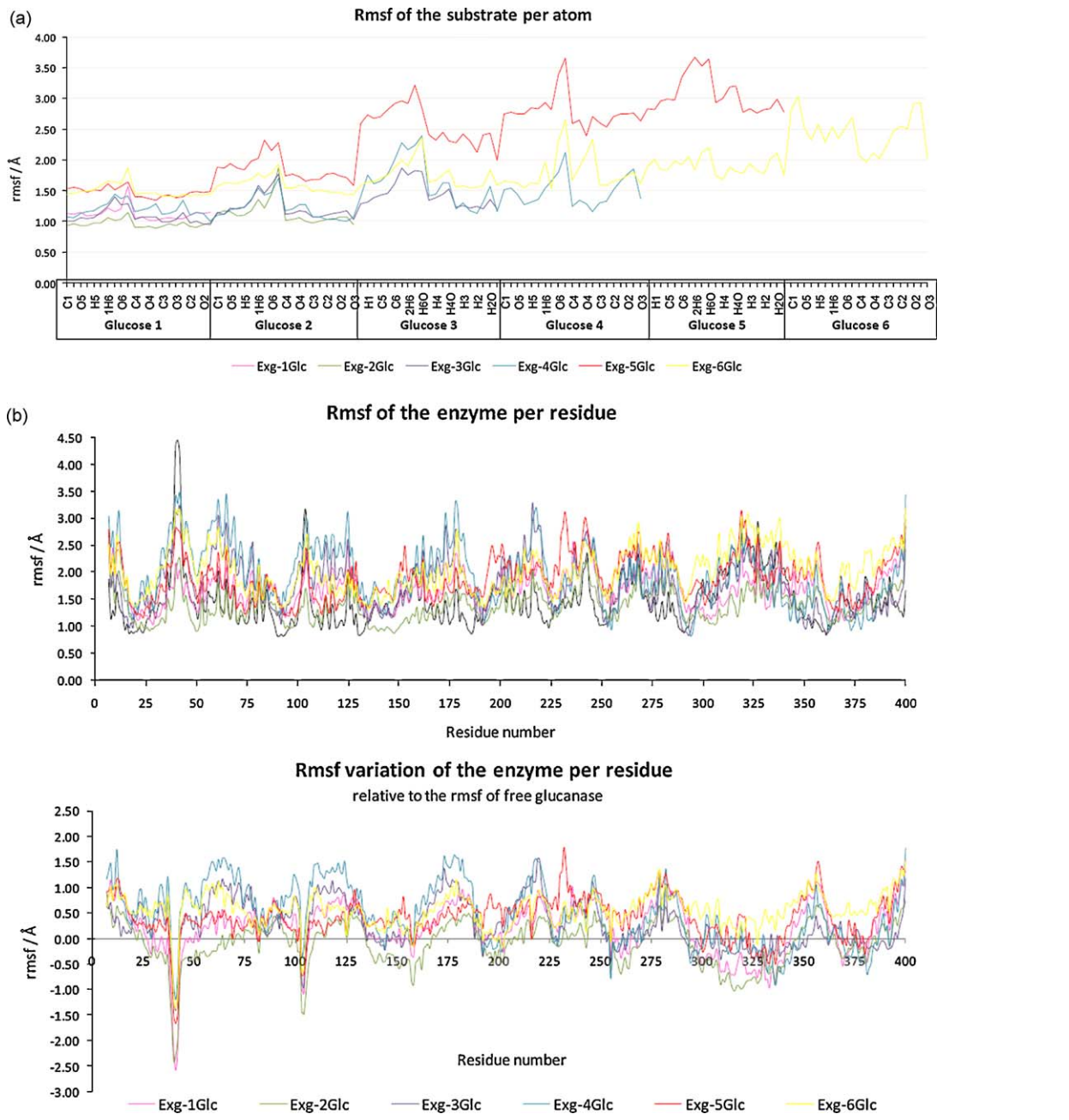

Fig. 4. (a) Rmsf per atom for the different substrates in complex with the enzyme. (b) Rmsf of the enzyme per residue: actual values (top) and rmsf variation in comparison to the free enzyme dynamics (bottom) in the different complexes during the 1000 ps production phase.

two terminal residues of a large polysaccharide chain before breaking the bond between them. Glucose residues 3–6 fluctuate more and the rmsf increases as the residue distance from the binding pocket augments, as expected. As already stated above, larger polysaccharide chains tend to create movement throughout the chain, corresponding to larger rmsf values for all residues; and this is particularly evident for the Exg–5Glc and Exg–6Glc complexes.

The rmsf per residue was calculated for all the enzyme structures and is shown in Fig. 4b (top). Observing the first chart, we can see that although the enzyme overall structure changes little over time (represented by constant rmsd values); individual amino acid residues can move significantly in space, represented by their relatively large rmsf values. The more rigid amino acids residues move only about 1 Å around their average structure, whereas amino acids in very flexible areas move as much as 4.5 Å. There is a stable pattern of fluctuation peaks and minima that probably correspond to surface and buried areas of the protein, respectively. Amino acid residues at the surface are freer to move, while residues confined to the interior of the protein have very little space to change conformation. The rmsf pattern and values are very similar for all Exg complexes, indicating that the enzyme behaves in a similar way, irrespective of the size of the substrate. Nevertheless, there are a few significant changes between the enzyme complexes and the free enzyme.

For a better assessment of how the enzyme structure is modified by substrate binding, the variation in the rmsf of each residue relative to the free enzyme structure was also calculated (Fig. 4b, bottom). The residue rmsf value for the free enzyme was subtracted from the residue rmsf of the enzyme in the substrate complexes to determine flexibility variations. We can observe in the graph that when a substrate was bound in the active site, the

enzyme registered increased movements (rmsf) of its residues, and this tendency is more evident for the larger substrates. It is likely that enzyme residues fluctuate more to accommodate the long flexible polysaccharide chain the protein is binding. There are, however, exceptions to this trend.

Examining the free enzyme rmsf, two large, clear peaks evidence themselves (Fig. 4b, top). The larger one is around amino acids 36–47 with a maximum of 4.46 Å in fluctuation for Gly41. The other peak has a maximum of 3.18 Å for Asp104 and refers to amino acids 101–106. When we calculate the variation in rmsf resulting from substrate binding (Fig. 4b, bottom) we observe that these two peaks become inverted peaks, indicating that there was a reduction in residue movement in these areas. The rmsf reduction varies from about −1 Å for Exg–2Glc to more than −2.5 Å for Exg–1Glc for the 36–47 peak. The variation is smaller for the 101–106 peak, but still negative. Recall that the free enzyme registered a conformational switch during dynamics, visible in the rmsd values, corresponding precisely to an observed change in conformation of the 36–47 loop. Repetition of this dynamics simulation and longer dynamics runs showed that this very sharp and swift conformational change was probably an unlikely event (results not shown). This kind of concerted movement of a large group of atoms usually takes many nanoseconds to be completed, and it was unusual that it occurred during the relatively short time of this dynamics run. However we chose to present this result here, since it brought to our attention the great flexibility of the 36–47 and 101–106 loops. The same rmsf peaks are observed for the other dynamics runs we conducted, although the conformational changes they indicate are not as visible (appearing as more gradual changes in rmsd). Results indicate that these loops are probably very flexible in the free enzyme, switching conformations over time. When a small substrate is bound in the active site one of the conformations of the loop might be stabilized, becoming more rigid. Our findings point to a possible biological role for these surface loops.

It is interesting to note that there is also a very broad peak in the region of a.a 291–361 of the rmsf chart. This corresponds to a large loop that is situated right next to the 36–47 loop, with a small gap between the two. The 291–361 loop has also a small reduction in flexibility upon substrate binding situated around amino acids 291–340, especially evident for the smaller substrates. This variation could be linked to the rmsf reduction registered in its neighbouring loop. Note also that the nucleophile residue (Glu292) is situated in this region.

The changes observed in the flexible loops mentioned were very interesting, and we decided to analyse their possible role a little further.

3.5. Modelling enzyme–polysaccharide binding in the flexible loops

First, several conformations of the loops were observed visually with Discovery Studio Visualizer (Fig. 5a). The free enzyme structure was observed both before (600 ps) and after (700 ps) the conformation changed. The rmsd between these two enzyme structures is only 0.93 Å. A large change was observed in loop 36–47 and smaller changes in loops 291–340 and 101–106 were also noted. Loop 36–47 changed from an "open" to a more "closed" conformation, closing the gap between this loop and loop 291–340 (Fig. 5a, I). Our observations suggest that the enzyme oscillates between these two conformations due to normal thermal motions, and one conformation may become more stable than the other after substrate binding. Additionally, the changes in loop flexibility seem to depend on the length and nature of the substrate. Note that the negative peak amplitude shown in Fig. 4b (bottom) generally decreases with the increase in substrate length. It is

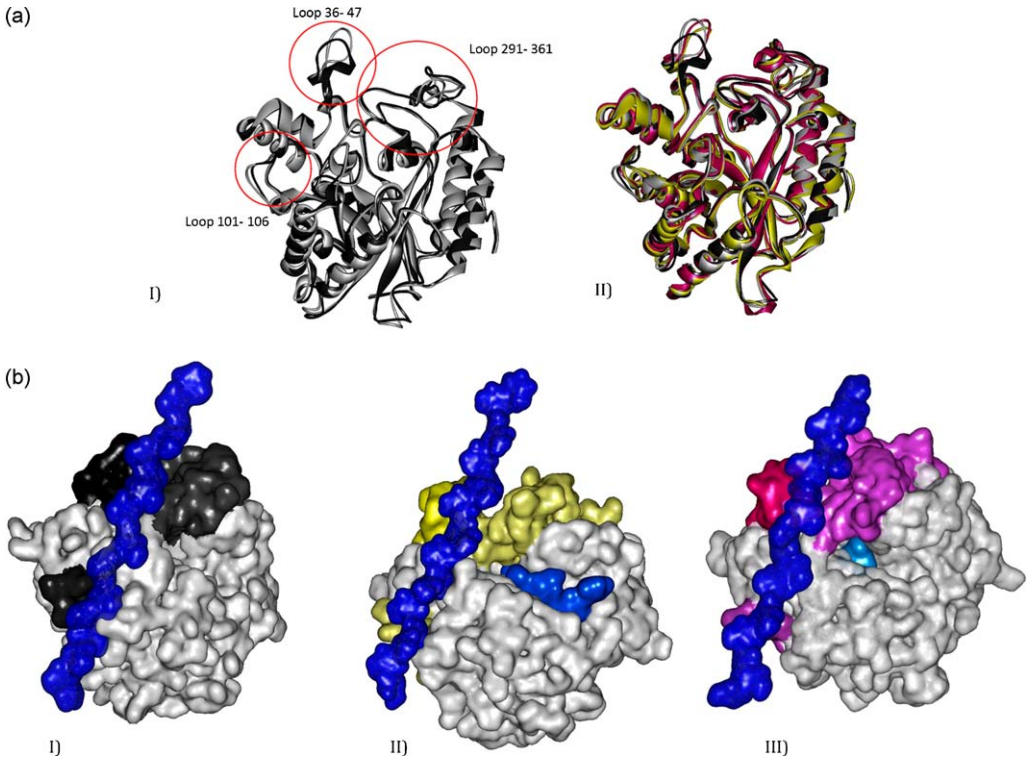

Fig. 5. (a) (I) Ribbons representation of the free Exg at 600 ps (grey) and 700 ps (black) of molecular dynamics. Note the change in conformation of the circled loops. The loops are named after the amino acid residues that comprise the peaks in enzyme rmsf. (II) Superimposition of various enzyme structures. Exg–6Glc at 500ps is in yellow and Exg–1Glc at 500 ps is pink, compared to the free Exg at 600 ps (grey) and 700 ps (black). A substantial variation is seen in the loops referred previously. (b) Results of enzyme:18Glc interaction modelling after structure optimization. The enzymes structures used are: (from left to right) free Exg (I), Exg–6Glc (II) and Exg–1Glc (III). Surface representation is used. The loops referred in (a) are singled out in colour.

Table 2
Summary of the interactions observed between the 18Glc polysaccharide ligand and the flexible enzyme loops and groove between them[a].

Complex	Interaction type	Loops 36–47/291–361	Groove	Loop 101–106
Exg:18Glc	H bridge	Asp43, Ser45	–	Ans105, Asp106 (2), Gly139, Asp159(2), Ans160, Gln162
	Dipole–dipole	–	–	Gln101, Asn154, Asn157
	London	–	Val49, Leu149	Leu103, Val163
Exg–6Glc:18Glc	H bridge	Arg309	Asp151, Ser152	Asp159
	Dipole–dipole	Asn42, Ans308, Arg309	Arg150	Asn157, Asn160
	London	–	Leu149	–
Exg–1Glc:18Glc	H bridge	Asn42 (3), Gln44, Ans308, Glu314	–	–
	Dipole–dipole	Asn308	–	–
	London	–	Val49	–

[a] Amino acids residues that interact with the ligand in more than one enzyme structure are highlighted.

therefore possible that for larger substrates than the ones studied here, the rmsf variation becomes positive.

The changes in loop structure were also studied for the enzyme–substrate complexes (Fig. 5a, II). The 6-Glc substrate should best represent the large glucan chains present in the cell wall, and is shown in the figure. The Exg–1Glc complex is also presented, since it is a product of the hydrolysis reaction, as well as a substrate for the transglucosylation reaction. Although the overall enzyme arrangement is virtually invariable for each structure observed, the flexible loops change conformation between the structures (Fig. 5a, II). The gap between loops 36–47 and 291–340 is smaller for the free glucanase structure and it becomes wider for the Exg–6Glc and Exg–1Glc structures.

The structure of the loops and their flexibility suggest they could be involved in binding a molecule on the surface of the protein. Since the most abundant substance in the cell wall is glucan polysaccharide chains, it seems more likely for the loops to bind one of these chains, if they are indeed designed for molecular binding. If the enzyme binds the cell wall in this way, it would not need to be glycosylated, explaining this unusual trait of the enzyme [10]. Therefore, we propose that the surface loops serve to bind the enzyme to the cell wall glucan. To test the plausibility of this model, a polysaccharide chain with 18 glucose residues linked by β-1,3 bonds (18Glc) was constructed and then bound to the enzyme using the loops and the groove that exists between them (external groove). The resulting structures were then optimized.

Fitting the 18Glc chain into the free glucanase was easy, since the two molecules were very complementary in shape, and the polysaccharide came into the gaps created by both sets of loops. The chain was placed with the 3-terminal closest to the 36–47 loop and the 1-terminal closest to the 101–106 loop (the alternative orientation was also tried, but found to be less favourable). After minimization, the enzyme structure changed very little (rmsd of 0.93 Å). As can be observed in Fig. 5b, I, the ligand chain was found to fit the enzyme particularly well, and it was held by loop 101–106. Some interactions are also made with the external groove and the 36–47 loop. A summary of all the interactions found by visual examination is presented in Table 2. Eight hydrogen bonds were established between the ligand and the region around loop 101–106; in addition some dipole-dipole and London interactions also were present. The remainder of the enzyme surface established fewer connections.

The way the enzyme and ligand shapes match each other, the several interactions established effortlessly between them, as well as the fact that neither enzyme nor ligand structure changed significantly during energy minimization seems to indicate that glucan binding to the surface loops can occur in reality. Although, naturally, experimental evidence is needed to support this theory.

Fitting the 18Glc chain onto the Exg–6Glc complex was also fairly straightforward, only a small rotation from the ligand position obtained in the previous structure was needed. After energy minimization, we observed that several enzyme–ligand interactions had also formed, but the way the enzyme held the polysaccharide chain changed. Both loop regions and groove equally interacted with 18Glc (Table 2).

Contrary to previous situations, it was very hard to fit 18Glc to the Exg–1Glc complex, due to the different conformation of the loops and the external groove, and it was necessary to significantly rotate the ligand chain. After structure optimization, some interactions were established between Exg and 18Glc in the loop 36–47 area, while only one London interaction was observed in the groove region and none in the 101–106 loop region (Table 2).

With this modelling procedure we discovered that it is potentially possible for the enzyme to bind to a glucan chain on its surface, and the way it binds could be changed as enzyme loops 36–47, 291–340 and 101–106 change conformation and flexibility. In the free Exg these loops are apparently very flexible, changing between an "open" and a "closed" structure (see Fig. 5a, I), that should be very close in energy since we can observe a reversible transition between the two states during the simulations. However, the binding of a small substrate chain in the active site of the enzyme could induce the stabilization of a given conformation of the loops. We observed different conformations of the loops when glucose and laminarihexaose were bound as substrates. These enzyme–substrate structures were also able to bind a glucan chain between the flexible loops, but the way the connection occurred was different for each structure used.

If the enzyme indeed binds the cell wall in the way proposed, the conformational and flexibility changes that occur with substrate binding could lead the enzyme to slide across a glucan chain or move laterally between chains as it binds, hydrolyses and releases the 3-terminal of another glucan chain.

According to experimental evidence, the transglucosylation reaction is faster than hydrolysis in high substrate concentrations [8]. The ability to slide along/move sideways between glucan chains in the tight glucan network would greatly facilitate the transglucosylation reaction, since the enzyme needs to cut a glucan chain and then quickly find another chain to bind the covalently linked glucose residue before it is released from the binding pocket.

4. Conclusions

Glycoside hydrolases are a very important group of enzymes, ubiquitous in nature [1]. With this work we intended to create an accurate model for polysaccharide–enzyme interaction to enhance the current understanding of the reaction mechanism and behaviour of these enzymes. β-1,3-Exoglucanase from the microorganism *C. albicans* was selected as a good computational model for family 5 glycosidases. Beginning with experimentally determined enzyme and enzyme–inhibitor complex structures we

were able to create several enzyme–substrate complexes, varying from one to six glucose residues. Structure optimization followed by molecular dynamics provided a more detailed understanding of the way the enzyme binds and holds its substrate over time.

Results obtained suggest that the enzyme structure is very rigid, especially around the active site, in agreement with experimental evidence [1]. The binding pocket appears to be designed to specifically bind and distort the 3-terminal glucose residue of a glucan chain, possibly providing also an extended charge relay system that facilitates the passage from the ground stage to the transition state structure together with protein–substrate binding. Our results indicate that the enzyme locks the two 3-terminal residues while slightly distorting the chain in order to position the scissile glycosidic bond in a favourable way for catalysis. The remainder of the glycosidic chain appears to interact more loosely with the binding groove, maintaining its hydration and intramolecular bonds. We propose that the binding groove could have a role in sliding the long laminari-chain into the binding pocket.

After substrate binding, the enzyme apparently becomes more flexible, probably because it is accommodating polysaccharide structure fluctuations. However, loops 36–47, 101–106 and 291–340, which were very flexible in the free Exg, became less flexible after the enzyme was bound to the different substrates studied here. This effect was very evident for the smaller substrates but it was reduced for the longer ones. The results point to a possible biological role for these loops and the hypotheses that the loops bind another glucan chain on the protein surface was explored. The results obtained sustain this model, since a laminari-type chain with 18 glucose residues showed to be surprisingly complementary to the enzyme structure in the loops region, and many interactions were established between the two molecules after structure optimization. We propose that the enzyme could bind the cell wall using these flexible loops and move along the wall as it undergoes the series of steps that comprise the reactions it catalyses. This is a totally novel model for the fixation of an enzyme to the cell wall, consistent with the absence of glycosylation, and experimental evidence is needed to support or refute this possibility.

Acknowledgments

The authors would like to thank the Portuguese Science and Technology Foundation (FCT-MCTES) for financial support (Scholarship SFRH/BD/36153/2007).

Appendix A. Supplementary data

Supplementary data associated with this article can be found, in the online version, at doi:10.1016/j.jmgm.2009.01.007.

References

[1] D.L. Zechel, S.G. Withers, Glycosidase mechanisms: anatomy of a finely tuned catalyst, Acc. Chem. Res. 33 (2000) 11–18.
[2] A. Vasella, G.J. Davies, M. Bohm, Glycosidase mechanisms, Curr. Opin. Chem. Biol. 6 (2002) 619–629.
[3] C.S. Rye, S.G. Withers, Glycosidase mechanisms, Curr. Opin. Chem. Biol. 4 (2000) 573–580.
[4] N.F. Bras, S.A. Moura-Tamames, P.A. Fernandes, M.J. Ramos, Mechanistic studies on the formation of glycosidase-substrate and glycosidase-inhibitor covalent intermediates, J. Comput. Chem. (2008).
[5] B. Henrissat, A classification of glycosyl hydrolases based on amino acid sequence similarities, Biochem. J. 280 (Pt 2) (1991) 309–316.
[6] H.M. Berman, J. Westbrook, Z. Feng, G. Gilliland, T.N. Bhat, H. Weissig, I.N. Shindyalov, P.E. Bourne, The protein data bank, Nucl. Acids Res. 28 (2000) 235–242.
[7] S.M. Cutfield, G.J. Davies, G. Murshudov, B.F. Anderson, P.C.E. Moody, P.A. Sullivan, J.F. Cutfield, The structure of the exo-beta-(1,3)-glucanase from *Candida albicans* in native and bound forms: relationship between a pocket and groove in family 5 glycosyl hydrolases, J. Mol. Biol. 294 (1999) 771–783.
[8] H.J. Stubbs, D.J. Brasch, G.W. Emerson, P.A. Sullivan, Hydrolase and transferase activities of the beta-1,3-exoglucanase of *Candida albicans*, Euro. J. Biochem. 263 (1999) 889–895.
[9] M. Osumi, The ultrastructure of yeast: cell wall structure and formation, Micron 29 (1998) 207–233.
[10] J.P. Lunaarias, E. Andaluz, J.C. Ridruejo, I. Olivero, G. Larriba, The major exoglucanase from *Candida albicans*—a nonglycosylated secretory monomer related to its counterpart from *Saccharomyces cerevisiae*, Yeast 7 (1991) 833–841.
[11] J. Nett, L. Lincoln, K. Marchillo, R. Massey, K. Holoyda, B. Hoff, M. VanHandel, D. Andes, Putative role of beta-1,3 glucans in *Candida albicans* biofilm resistance, Antimicrob. Agents Chemotherapy 51 (2007) 510–520.
[12] M.D. Gonzalez, R. DiezOrejas, G. Molero, A.M. Alvarez, J. Pla, C. Nombela, M. SanchezPerez, Phenotypic characterization of a *Candida albicans* strain deficient in its major exoglucanase, Microbiology, UK 143 (1997) 3023–3032.
[13] D.A. Case, T.E. Cheatham, T. Darden, H. Gohlke, R. Luo, K.M. Merz, A. Onufriev, C. Simmerling, B. Wang, R.J. Woods, The Amber biomolecular simulation programs, J. Comput. Chem. 26 (2005) 1668–1688.
[14] J.M. Wang, R.M. Wolf, J.W. Caldwell, P.A. Kollman, D.A. Case, Development and testing of a general amber force field, J. Comput. Chem. 25 (2004) 1157–1174.
[15] G. Jones, P. Willett, R.C. Glen, Molecular recognition of receptor-sites using a genetic algorithm with a description of desolvation, J. Mol. Biol. 245 (1995) 43–53.
[16] M.L. Verdonk, J.C. Cole, M.J. Hartshorn, C.W. Murray, R.D. Taylor, Improved protein–ligand docking using GOLD, Proteins-Struct. Funct. Gen. 52 (2003) 609–623.
[17] M.J. Hartshorn, M.L. Verdonk, G. Chessari, S.C. Brewerton, W.T.M. Mooij, P.N. Mortenson, C.W. Murray, Diverse, high-quality test set for the validation of protein–ligand docking performance, J. Med. Chem. 50 (2007) 726–741.
[18] J.W. Liebeschuetz, Evaluating docking programs: keeping the playing field level, J. Comp-Aided Mol. Design 22 (2008) 229–238.
[19] S.G. Lambrakos, J.P. Boris, E.S. Oran, I. Chandrasekhar, M. Nagumo, A Modified shake algorithm for maintaining rigid bonds in molecular-dynamics simulations of large molecules, J. Comput. Phys. 85 (1989) 473–486.
[20] J.A. Izaguirre, D.P. Catarello, J.M. Wozniak, R.D. Skeel, Langevin stabilization of molecular dynamics, J. Chem. Phys. 114 (2001) 2090–2098.
[21] W. Humphrey, A. Dalke, K. Schulten, VMD: visual molecular dynamics, J. Mol. Graphics 14 (1996), 33.
[22] Woods_Group. Biomolecule Builder, in: GLYCAM Web: Complex Carbohydrate Research Center, The University of Georgia.
[23] X. Biarnes, A. Ardevol, A. Planas, C. Rovira, A. Laio, M. Parrinello, The conformational free energy landscape of beta-D-glucopyranose. Implications for substrate preactivation in beta-glucoside hydrolases, J. Am. Chem. Soc. 129 (2007) 10686–10693.
[24] J. Tooze, B. Carl, An example of enzyme catalysis: serine proteinases, in: Introduction to Protein Structure, Garland Science Publishing, New York, 1999, pp. 205–213.
[25] K. Denker, F. Orlik, B. Schiffler, R. Benz, Site-directed mutagenesis of the greasy slide aromatic residues within the LamB (maltoporin) channel of *Escherichia coli*: effect on ion and maltopentaose transport, J. Mol. Biol. 352 (2005) 534–550.